Analysis of Leg-Open Fault of Three-Phase Delta-Delta LLC Resonant Converter

Hyun-Jin Jin, Jihun So, Yoo-Seop Kim, Yeong-Jun Choi

Analysis of Leg-Open Fault of Three-Phase Delta-Delta LLC Resonant Converter

Hyun-Jin Jin, Jihun So, Yoo-Seop Kim and Yeong-Jun Choi†
Department of Electrical Engineering, Jeju National University
102 Jejudaehak-ro, Jeju-si, Jeju-do 63243, South Korea
Jeju, South Korea
Tel.: +82 / (64) – 754.3677.
E-Mail: dkswpffk1219@jejunu.ac.kr, jihun.so@stu.jejunu.ac.kr, rdgcw12@jejunu.ac.kr,
†yeongjun.choi@jejunu.ac.kr

Acknowledgements

This work was supported by the National Research Foundation of Korea(NRF) grant funded by the Korea government(MSIT) (RS-2024-00405278).

Keywords

«Fault operation», «LLC resonant converter», «Reliability», «Open switch fault», «Output voltage recovery».

Abstract

Highly reliable LLC resonant converters operating even under fault conditions are important in aerospace, data center, and electrolyzer applications that require continuous and stable power supply. Therefore, analyzing the operating characteristics and researching methods for maintaining output voltage is essential. Thus, this paper analyzes the operation mode and resonant characteristics of a three-phase delta-delta LLC resonant converter after faults, focusing on open-circuit faults. Based on the analysis, equivalent circuits and voltage gain curves after the faults are derived and compared with those before the faults. The decreased output voltage due to the faults are recovered through PFM(Pulse Frequency Modulation). Consequently, the output voltage is recovered without additional components, and it is intuitively interpreted that the operating frequency is adjusted to achieve voltage gain as the resonant frequency changes after the faults. The analysis results are verified by PLECS simulation.

Introduction

With the spread of renewable energy sources and the electrification of transportation, isolated DC/DC converters that stably convert power between high and low voltages are playing an important role. Among them, LLC resonant converters are widely used due to their features such as soft switching, high efficiency, and high power density[1]-[4]. In particular, applications such as aerospace, data centers and electrolyzers require highly reliable power conversion devices that supply continuous and stable dc power[5]-[8].

However, power converters often fail while converting and transferring energy. These faults are caused by components that make up power electronic converters such as power semiconductors and resonant capacitors[9]. In various fault types, switch failure is the most common fault in the power electronic converter[10]. The major causes of the switch failure are overvoltage, overcurrent, and overheating, with possible fault types including open-circuit faults and short-circuit faults[10]-[12]. In general, most faults result in open-circuit faults[10],[11]. If an open-circuit fault occurs in a switch of a leg, the voltage and current stress on the remaining components may become more severe, potentially causing abnormal operation of the healthy switches[11]. This leads to another switch failure, resulting in the leg open fault.

Due to these faults, the power converter cannot maintain the output voltage. This causes power supply interruption and leads to many consequences such as safety issues and increased operating costs. Therefore, it is essential to analyze the operation of LLC resonant converters and research methods for maintaining output voltage when faults occur. Accordingly, research on LLC resonant converters operating with faults has been actively conducted[13]-[15].

Based on previous research, unlike single-phase LLC resonant converters, multiphase LLC resonant converters continue operating even under fault conditions by reconfiguring the topology and employing PFM(Pulse Frequency Modulation) without additional components. Moreover,

multiphase LLC resonant converters exhibit low output current ripple, which allows for decreased output capacitor size and prevents efficiency degradation in the load devices[16],[17].

Among the multiphase LLC resonant converters, the three-phase LLC resonant converter is mainly adopted because it is relatively cost-effective[18]. The three-phase LLC resonant converter is divided into wye-type and delta-type according to the transformer connection. The delta-type connection has an advantage in realizing high power density due to low transformer losses[18],[19]. This feature applies even when a switch fault occurs on one leg. Structurally, in the delta-type connection, current flows through all phases of the transformer after leg-open faults. Whereas, in the wye-type connection, current flows only through the transformer connected to the healthy leg after the leg-open faults. Consequently, there is considerably less current flowing in the transformer of a three-phase delta-type LLC resonant converter after a leg-open fault. In this circuit, to maintain the output voltage under faulty operating conditions, it is necessary to analyze the operation mode after the fault. However, there is not enough research on three-phase delta-delta LLC resonant converters after leg-open fault.

Therefore, this paper analyzes the operating mode and resonant tank characteristics of a three-phase delta-delta LLC resonant converter after the leg-open fault. In addition, PFM is utilized to recover the decreased output voltage due to the faults.

As a result, the decreased output voltage on the output side is recovered without additional components. Also, the analysis provides a basis for an intuitive interpretation of the PFM by analyzing the operation mode and identifying the resonant frequency and Q factor after the faults. Finally, the analysis results are verified through PLECS simulation and confirmed the operation mode and resonant characteristics after the fault.

Circuit Description

The three-phase delta-delta LLC resonant converter consists of primary switches $S_1 \sim S_6$, resonant tanks, transformers $T_A \sim T_C$ and secondary diodes $D_1 \sim D_6$ as shown in Fig. 1. The upper and lower switches on the same leg operate complementary. The upper switches S_1, $S_3$and S_5 have 120° phase shift. Similarly, the lower switches S_2, $S_4$and S_6 have 120°phase shift. The resonant tanks are composed of resonant

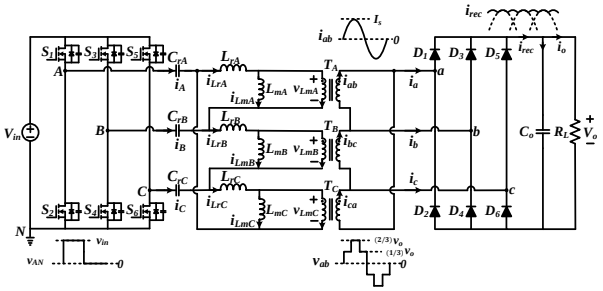

Fig. 1 Three-phase delta-delta LLC resonant converter.

capacitances $C_{rA} \sim C_{rC}$, resonant inductances $L_{rA} \sim L_{rC}$, and magnetizing inductances $L_{mA} \sim L_{mC}$. The resonant currents are $i_{LrA} \sim i_{LrC}$ and the magnetizing currents are $i_{LmA} \sim i_{LmC}$. The resonant tanks input voltages are $v_{AN} \sim v_{CN}$.

The primary and secondary sides are connected to transformer with a delta-type connection. The phase voltages of the primary transformer are $v_{LmA} \sim v_{LmC}$ and the secondary phase voltages are v_{ab}, v_{bc} and v_{ca}. The phase currents flowing in the primary transformer are i_{AB}, i_{BC} and i_{CA}. The secondary phase currents are i_{ab}, i_{bc} and i_{ca} respectively. The primary line currents, which are also the capacitor currents, are i_A, i_B, and i_C. The secondary line currents are i_a, i_b, and i_c.

Operation Mode Analysis

The main waveforms of the three-phase LLC delta-delta resonant converter before and after the leg-open fault are presented and each mode of operation is explained in this section. In particular, after the fault, the circuit is no longer balanced, so the waveforms for each phase are depicted separately. The key waveforms are shown with the

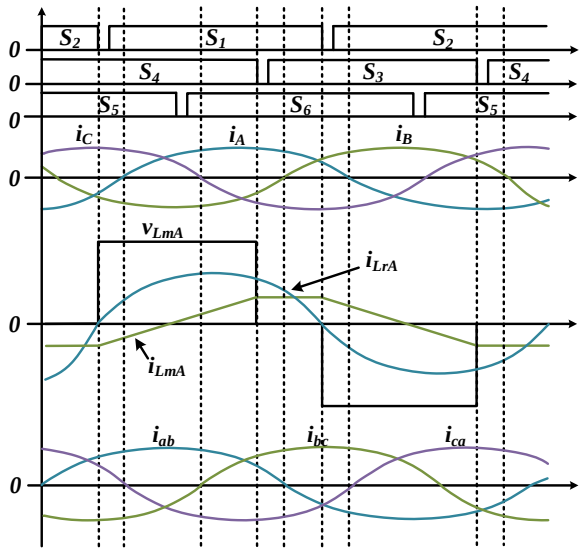

Fig. 2 Key waveforms of pre-fault operation.

primary line current, phase voltage, resonant current, magnetizing current, and secondary phase current.

A. Pre-Fault Operation Mode

The main waveforms of the three-phase delta-delta LLC resonant converter before the leg-open fault are shown in Fig. 2. Before the faults, the switching frequency is equal to the resonant frequency. If the three-phase circuit is balanced, one phase is identical to the other two phases with phases shifted by 120° each other. In a three-phase converter, the phase voltage of the transformer is three levels, which is applied to the magnetizing inductance. In the resonant tank, i_{LmA} is increasing while a positive voltage is applied to the magnetizing inductance and i_{LmA} is decreasing while a negative voltage is applied to the magnetizing inductance. In the interval where the v_{LmA} is zero, i_{LmA} is constant as depicted in Fig. 2. When the i_{LrA} goes from zero to positive, v_{LmA} becomes positive. Likewise, i_{LrA} goes from zero to negative, v_{LmA} becomes negative.

B. After Leg-Open Fault Operation Mode

The key waveforms after the leg-open fault are shown in Fig.3 and Fig.4. Fig.3 shows the key waveforms of the current flowing though T_A, while Fig.4 illustrates the key waveforms of the current flowing through T_B and T_C. The key waveforms are divided into six modes. When the open fault occurs in leg C, i_C no longer flows in the circuit and i_A becomes equal to i_B. This means that since the i_C does not flow, i_A flows through the transformer, and that current directly comes out as i_B.

However, phase current, resonant current, and magnetizing current still flow through all phases inside the transformer. Compared to pre-fault operation, i_{ab} increases, while i_{bc}, i_{ca} decrease. As i_C does not flow due to the fault in C leg, the current distribution within delta transformer is also changed. Consequently, v_{TB} and v_{TC} are connected in series, so the current flowing through v_{TB} also flows identically through v_{TC}. Also, half of the current flowing through v_{TA} flows through v_{TB} and v_{TC} with phase shifted by 180°. As shown in Fig. 3 and Fig. 4, v_{LmA} decreases and changes to two levels. At t_5 to t_6, the resonant current and the magnetizing current become equal. During this interval, transformers are stopped transmitting energy from the primary side to the secondary side. This indicates that, after the faults,

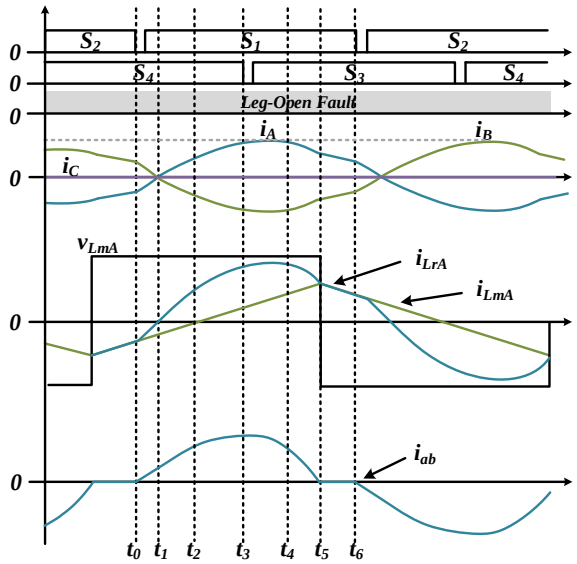

Fig. 3 Key waveforms in T_A after Leg-Open fault operation.

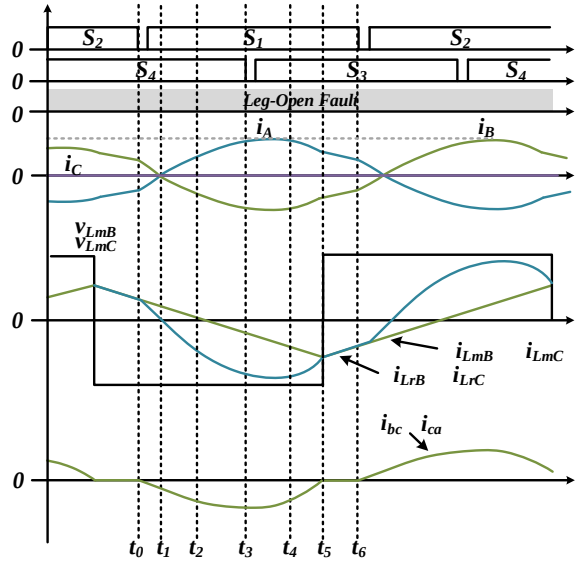

Fig. 4 Key waveforms in T_B and T_C after Leg-Open fault operation.

the switching frequency is lower than the resonant frequency. The operating characteristics of the current flowing in the resonant tank are the same as the phase current. That is, i_{LrA} and i_{LmA} flowing in T_A are twice the current flowing in T_B and T_C with phase shifted by 180°.

Since the operating characteristics of the primary side are also applied to the secondary side, i_c cannot flow through the diode of leg c. As a result, the after-fault circuit is not balanced. Therefore, operation mode analysis for each phase is required. In order to analyze the operation mode in detail, as shown in Fig. 4, the subcircuits for each operation mode are presented.

(1) Mode1 [$t_0 \leq t < t_1$]

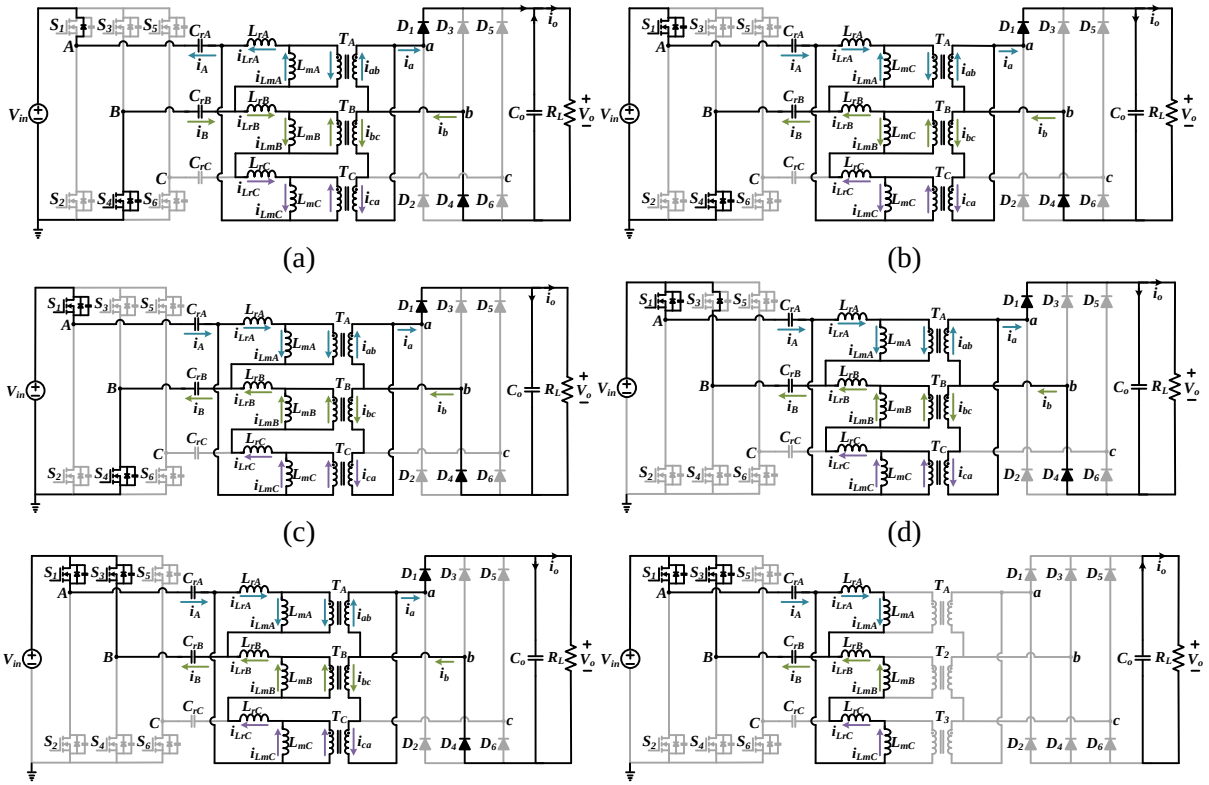

Fig. 4 Subcircuits for each operation mode. (a) mode1 [$t_0 \le t < t_1$], (b) mode2 [$t_1 \le t < t_2$], (c) mode3 [$t_2 \le t < t_3$], (d) mode4 [$t_3 \le t < t_4$], (e) mode5 [$t_4 \le t < t_5$], (f) mode6 [$t_5 \le t < t_6$].

S_2 is turned off at t_0 and S_4 remains on. The leakage inductance resonates with resonant capacitance. During the dead time, negative current i_A flows before S_1 turns on, achieving soft switching condition. At the end of the dead time, i_A still flows in the negative direction through S_1. The operation for mode1 is shown in Fig.4(a).

(2) Mode2 [$t_1 \le t < t_2$]

S_4 remains on and S_1 achieves ZVS-on(Zero Voltage Switching-on). At t_1, i_A and i_{LrA} are changed from negative to positive. The primary phase currents flow to the secondary side through transformers transmitting energy, as shown in Fig.4(b).

(3) Mode3 [$t_2 \le t < t_3$]

S_1 and S_4 remain on. At t_2, the i_{LmA} is changed from negative to positive. The current flowing in the resonant tank of T_A is gradually increased. At t_3, the S_4 is turned off. The operation for mode3 is shown in Fig.4(c).

(4) Mode4 [$t_3 \le t < t_4$]

S_4 turns off at t_3 and S_1 remains on. During mode4, i_A and i_{LrA} flow has the largest current magnitude among the six modes. During mode4, power is transferred to the secondary through a transformer as shown in Fig. 4(d).

(5) Mode5 [$t_4 \le t < t_5$]

S_1 and S_3 remain on. During mode5, i_A and i_{LrA} are gradually decreased. Accordingly, i_{ab} is also decreased. The operation for mode5 is shown in Fig.4(e).

(6) Mode6 [$t_5 \le t < t_6$]

The switch state remains the same as in mode5. The magnetizing inductance participates in the resonance at t_6. As a result, the i_{LrA} and i_{LmA} becomes equal. The transformers stop transmitting energy to the secondary side as shown in Fig.4(f).

Analysis of Voltage Gain

The voltage gain is a parameter that reflects the output characteristics of the LLC resonant converter. To analyze voltage gain, the FHA(Fundamental Harmonic Approximation) equivalent circuit is obtained, and the gain equation is derived.

A. FHA Equivalent Circuit

To express the three-phase delta-delta LLC resonant converter, the delta-wye transformation is used. Thus, the delta connection of the primary side is replaced with a wye connection to represent

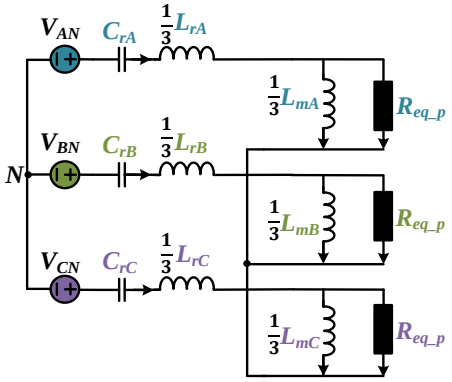

Fig. 5 Three-phase equivalent circuit of delta-delta LLC Resonant converter.

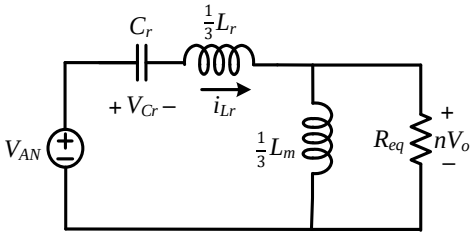

Fig. 6 Single-phase FHA equivalent circuit.

a three-phase LLC resonant converter equivalent circuit as shown in Fig.5. If the three-phase circuit is balanced, a single-phase FHA equivalent circuit is extracted separately as shown in Fig. 6.

The input voltage v_{AN} of the resonant tank is equal to (1) by applying FHA. ω_s is the switching frequency.

$$v_{AN} = \frac{2V_{in}}{\pi}\sin(\omega_s t) \tag{1}.$$

To represent the secondary equivalent load resistance R_{eq_s}, the secondary phase voltage v_{ab}, output current i_o, line current i_a, and phase current i_{ab} are obtained by (2)-(5), respectively.

$$V_{ab} = \frac{2\sqrt{3}}{\pi}V_o\sin(\omega_s t + \frac{\pi}{6}) \tag{2}.$$

$$I_o = \frac{6\omega_s}{2\pi}\int_{\frac{\pi}{3}}^{\frac{2\pi}{3}} I_a \sin(\omega_s t + \frac{\pi}{6}) \tag{3}.$$

$$I_a = \frac{\pi}{3}I_o \tag{4}.$$

$$I_{ab} = \frac{\pi}{3\sqrt{3}}I_o \tag{5}.$$

Consequently, R_{eq_s} is expressed by (6), and considering the transformer turns ratio $n = \frac{N_p}{N_s}$, the secondary equivalent load resistance with respect to the primary R_{eq_p} is expressed by (7).

$$R_{eq\_s} = \frac{V_{ab}}{I_{ab}} = \frac{18V_o}{\pi^2 I_o} = \frac{18}{\pi^2}R_L \tag{6}.$$

$$R_{eq\_p} = (\frac{N_p}{N_s})^2 R_{eq\_s} = \frac{18n^2}{\pi^2}R_L \tag{7}.$$

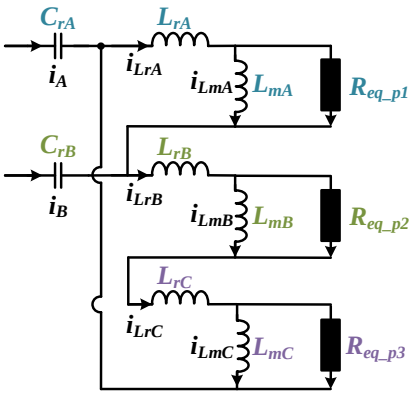

Fig. 7 Equivalent circuit after leg-open fault.

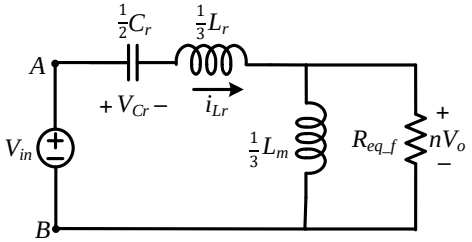

Fig. 8 After leg-open fault FHA equivalent circuit.

By applying the delta-wye transformation, L_r, C_r, L_m, and R_{eq} for single phase are expressed as (8) to (11).

$$C_r = C_{rA} \tag{8}.$$

$$L_r = \frac{L_{rA}}{3} \tag{9}.$$

$$L_m = \frac{L_{mA}}{3} \tag{10}.$$

$$R_{eq} = \frac{R_{eq\_p}}{3} = \frac{6n^2}{\pi^2}R_L \tag{11}.$$

The three-phase equivalent circuit after the leg-open fault is shown in Fig.7. Since the three-phase circuit is unbalanced, FHA is applied to the voltage and current of each phase.

The input voltage v_{AN} on the primary side is equal to (1). According to the operation mode analysis, R_{eq_p2} and R_{eq_p3} are the same, and the current and voltage flowing through T_B and T_C are also the same. Therefore, only the current and voltage flowing in T_A, T_B are expressed. The secondary phase voltage and output current are obtained by (13)-(15). The line current and phase current of the secondary side are obtained by (16)-(18) respectively.

$$V_{ab} = \frac{2\sqrt{3}}{\pi}V_o\sin(\omega_s t + \frac{\pi}{6}) \tag{13}.$$

$$V_{bc} = \frac{\sqrt{3}}{\pi}V_o\sin(\omega_s t + \frac{\pi}{6}) \tag{14}.$$

$$I_o = \frac{2\omega_s}{2\pi}\int_0^{\frac{5\pi}{6}} I_a \sin(\omega_s t + \frac{\pi}{6}) \quad (15).$$

$$I_a = \pi I_o \quad (16).$$

$$I_{ab} = \frac{2}{3} I_a \quad (17).$$

$$I_{bc} = \frac{1}{3} I_a \quad (18).$$

Consequently, R_{eq_1s} and R_{eq_2s} are expressed to (19) and (20). The secondary equivalent load resistances for the primary R_{eq_p1}, R_{eq_p2} are equal to (21) and (22), considering the transformer turn ratio.

$$R_{eq\_1s} = \frac{V_{ab}}{I_{ab}} = \frac{3\sqrt{3}V_o}{\pi^2 I_o} = \frac{3\sqrt{3}}{\pi^2} R_L \quad (19).$$

$$R_{eq\_2s} = \frac{V_{bc}}{I_{bc}} = \frac{3\sqrt{3}V_o}{\pi^2 I_o} = \frac{3\sqrt{3}}{\pi^2} R_L \quad (20).$$

$$R_{eq\_p1} = (\frac{N_p}{N_s})^2 R_{eq\_1s} = \frac{3\sqrt{3}n^2}{\pi^2} R_L \quad (21).$$

$$R_{eq\_p2} = (\frac{N_p}{N_s})^2 R_{eq\_2s} = \frac{3\sqrt{3}n^2}{\pi^2} R_L \quad (22).$$

Through the (19)-(22), the secondary equivalent resistance is the same for each phase after the leg-open fault occurs and is obtained as (23).

$$R_{eq\_f} = \frac{3\sqrt{3}n^2}{\pi^2} R_L \quad (23).$$

After the leg-open fault, all three phases of the transformer are activated, so the inductance is the same as before the fault. Equivalent inductance L_{r_f} is equal to (24). Resonant capacitances C_{r1} and C_{r2} are connected in series, so the equivalent resonant capacitance C_{r_f} is equal to (25). Equivalent magnetizing inductance is equal to (26).

$$L_{r\_f} = \frac{1}{3} L_{rA} \quad (24).$$

$$C_{r\_f} = \frac{1}{2} C_{rA} \quad (25).$$

$$L_{m\_f} = \frac{1}{3} L_{mA} \quad (26).$$

As a result, the equivalent circuit of a three-phase delta-delta LLC resonant converter after a leg-open fault is obtained as depicted in Fig. 8.

B. Voltage Gain Curve

The voltage gain equation is expressed by the equivalent circuit. Based on the FHA equivalent circuit shown in Fig. 6, the voltage gain equation of the pre-fault three-phase delta-delta LLC resonant converter is expressed as (27). By rearranging (27), the voltage gain is finally obtained as (28).

$$M(j\omega_s) = \left\| \frac{j\omega_s L_m || R_{eq}}{j\omega_s L_m || R_{eq} + j\omega_s L_r + \frac{1}{j\omega_s C_r}} \right\| \quad (27).$$

Where Q is the quality factor, ω_x is the normalized frequency, ω_s is the switching frequency, ω_o is the resonant frequency and m is the ratio of the magnetizing inductance to the resonant inductance.

$$M(j\omega_s)_{\Delta-\Delta} = \frac{\omega_x^2(m-1)}{\sqrt{(m\omega_x^2-1)^2 + Q^2\omega_x^2(\omega_x^2-1)^2(m-1)^2}} \quad (28).$$

$$Q = \frac{1}{R_{eq}}\sqrt{\frac{L_r}{C_r}} = \frac{1}{R_{eq}}\frac{1}{\sqrt{3}}\sqrt{\frac{L_{r\mathrm{A}}}{C_{r\mathrm{A}}}} \quad (29).$$

$$\omega_x = \frac{\omega_s}{\omega_o} \quad (30).$$

$$\omega_o = \frac{1}{\sqrt{L_r C_r}} = \frac{\sqrt{3}}{\sqrt{L_{rA} C_{rA}}} \quad (31).$$

$$m = \frac{L_r + L_m}{L_r} \quad (32).$$

In the same way, according to the FHA equivalent circuit shown in Fig. 8, the voltage gain after a leg-open fault is obtained as (33).

Where, Q_f is quality factor, ω_{x_f} is the normalized frequency, ω_{o_f} is the resonant frequency and m_f is the ratio of the magnetizing inductance to the resonant inductance after the faults, respectively.

$$M(j\omega_s)_{\Delta-\Delta_f} = \frac{{\omega_{x\_f}}^2(m\_f-1)}{\sqrt{(m\_f{\omega_{x\_f}}^2-1)^2 + Q\_f^2{\omega_{x\_f}}^2({\omega_{x\_f}}^2-1)^2(m\_f-1)^2}} \quad (33).$$

$$Q\_f = \frac{1}{R_{eq\_f}}\sqrt{\frac{L_{r\_f}}{C_{r\_f}}} = \frac{1}{R_{eq\_f}}\frac{\sqrt{2}}{\sqrt{3}}\sqrt{\frac{L_{r\mathrm{A}}}{C_{r\mathrm{A}}}} \quad (34).$$

$$\omega_{x\_f} = \frac{\omega_s}{\omega_{o\_f}} \quad (35).$$

$$\omega_{o\_f} = \frac{1}{\sqrt{L_{r\_f} C_{r\_f}}} = \frac{\sqrt{6}}{\sqrt{L_{rA} C_{rA}}} \quad (36).$$

$$m_f = \frac{L_{r\_f} + L_{m\_f}}{L_{r\_f}} \quad (37).$$

As shown in (28) and (33), the voltage gain is determined by the transformer turns ratio, inductance ratio, normalized frequency, and Q.

Therefore, the voltage gain after the faults decreases as the Q increases as shown in (29) and (34). The resonant frequency after the faults changes and becomes $\sqrt{2}$ times larger than the resonant frequency in pre-fault operation. This is also presented in Fig. 9. Comparing the resonant

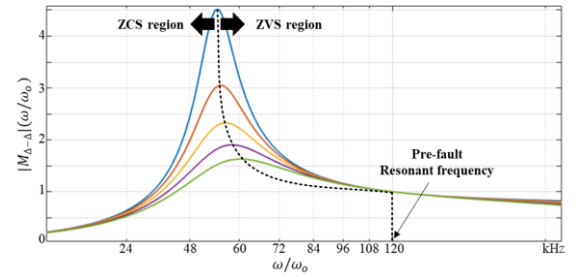

(a)

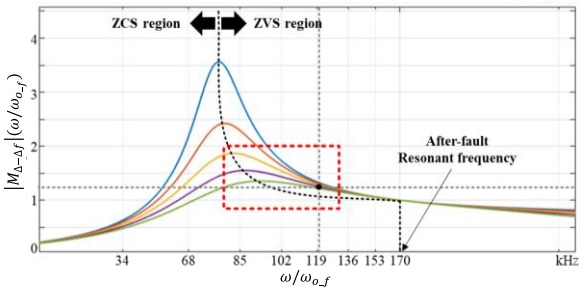

(b)

Fig. 9 Voltage gain curves. (a)pre-fault operation, (b) after leg-open fault.

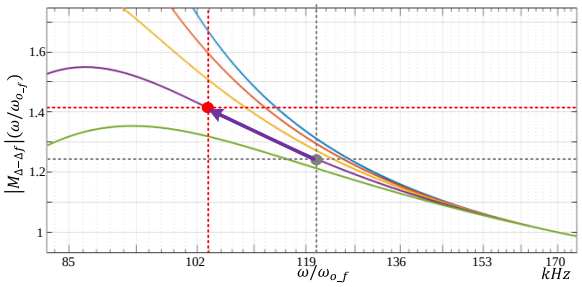

Fig. 10 Enlarged voltage gain curves after leg-open fault.

frequency on the gain curve before the fault in Fig. 9(a) with the resonant frequency on the gain curve after the fault in Fig. 9(b) reveals that the resonant frequency increases after the fault occurs. Therefore, the pre-fault resonant frequency is included in the below resonance region, which indicates by the black point as shown in Fig. 9(b). This is because the inductance of the transformer remains the same and the capacitance becomes smaller after the faults due to the delta connection. This relationship of the resonant frequency before and after the faults also are expressed by (31) and (36). In both Fig. 9(a) and Fig. 9(b), the voltage gain at the resonant frequency is unity.

However, as mentioned above, the resonant frequency increases and the output voltage drops during the leg-open fault. Accordingly, compared with the voltage gain of the pre-fault operation, after a leg-open fault, the voltage gain at resonant frequency decreases.

Therefore, the switching frequency must be adjusted in order to maintain the output voltage before the faults. Fig. 10 is an enlarged area marked with a box in Fig. 9(b). In Fig. 10, the black point is the pre-fault resonant frequency. From the black point, the switching frequency is moved to the red point to maintain the output voltage. Therefore, after the open-circuit fault, the three-phase delta-delta LLC resonant converter

Table I: Three-Phase Delta-Delta LLC Resonant Converter Parameters

Symbol	Parameter	Value
V_{in}	Input voltage	400 V
V_o	Output voltage	48 V
P_o	Output power	2 kW
f_s	Switching frequency	120 kHz
f_r	Resonant frequency	120 kHz
L_m	Magnetizing inductance	240 µH
L_r	Leakage inductance	60 µH
C_r	Resonant capacitance	87.3 nF

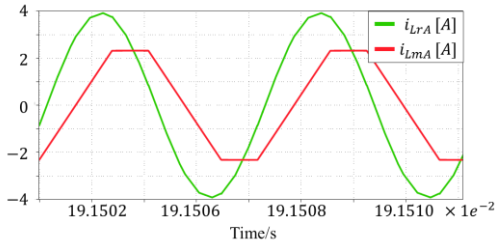

(a)

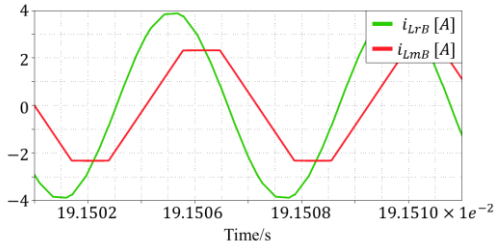

(b)

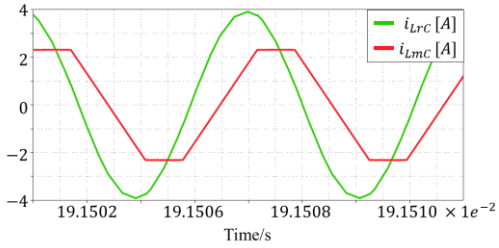

(c)

Fig. 11 Simulation results for pre-fault operation (a) resonant currernt and magnetizing current flowing in T_A (b) resonant currernt and magnetizing current flowing in T_B (c) resonant currernt and magnetizing current flowing in T_C

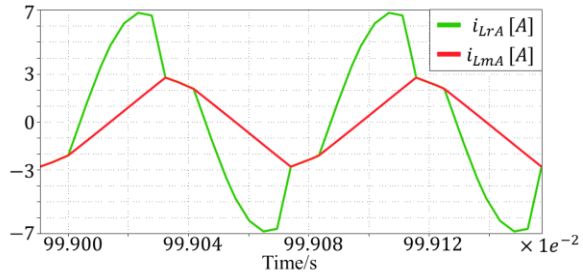

(a)

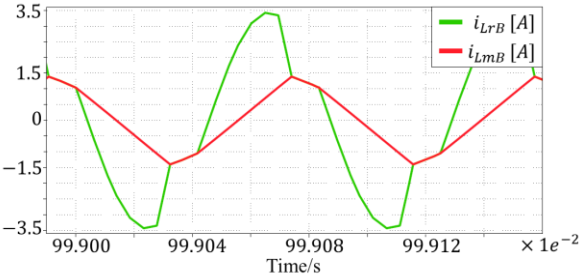

(b)

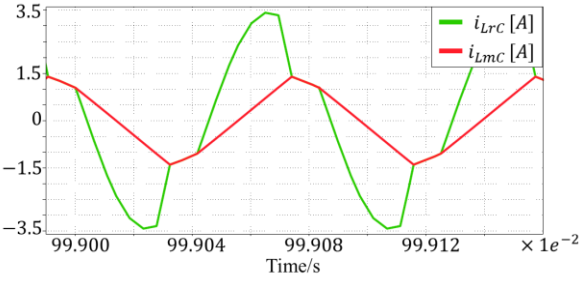

(c)

Fig. 12 Simulation results after the fault operation (a) resonant currernt and magnetizing current flowing in T_A (b) resonant currernt and magnetizing current flowing in T_B (c) resonant currernt and magnetizing current flowing in T_C

operates at switching frequency lower than the resonant frequecy after the fault.

Simulation Results

The simulation parameters for verifying the analysis of the three-phase delta-delta LLC resonant converter are shown in Table I. Before the faults occurred, the converter operates at the resonant frequency 120 kHz.

Fig. 11 shows the waveforms for the resonant and magnetizing currents of a resonant circuit flowing in each phase. The currents in each phase are flowing with phase shifted by 120° and switching frequency operates at the resonant frequency. The magnetizing current is constant in the interval where the voltage across the magnetic inductance is zero.

After leg-open fault occurs, the converter operates at the below resonant frequency as shown in Fig. 12. Fig. 12(a) is the resonant and

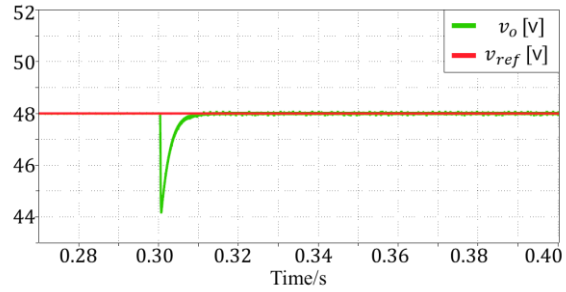

(a)

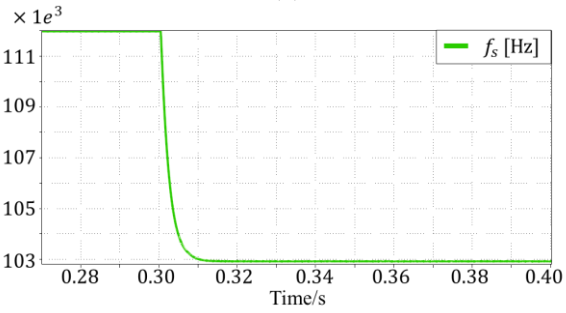

(b)

Fig. 13 Simulation results (a) output voltage, (b) switching frequency

magnetizing currents flowing in T_A. Fig. 12(b) and Fig. 12(c) are the resonant and magnetizing currents flowing in T_B and T_C, respectively, and are in phase with each other. However, they are 180° phase shift with the resonant and magnetizing currents flowing in T_A. Moreover, the resonant current and magnetizing current flowing through T_B and T_C is half of the current flowing through T_A.

Fig. 13 shows the recovered output voltage achieved by adjusting the swtiching frequency using PFM after the leg-open fault. the voltage and frequency. As shown in Fig. 13(a), At 0.3s, a leg-open fault occurs and the output voltage drops to 44 V. At this point, the switching frequency decrease to 103 kHz so that the output voltage is 48 V as shown in Fig. 13(b). It was confirmed that the resonant frequency after the faults is higher than pre-fault. This also means that the switching frequency after the faults is lower than the resonant frequency.

Conclusion

In this paper, when a leg-open fault occurs, the operation mode and resonance characteristics of a three-phase delta-delta LLC resonant converter are analyzed. After the leg-open faults, no current flows through the faulty leg, however, current flows through all phases of the transformer. Additionally, before the fault occurs, the

switching frequency operates at the resonant frequency, whereas after the fault, it operates below resonant frequency. Consequently, it is confirmed that the resonant frequency and Q change after the leg-open fault occurs. Resonant frequency during a leg-open fault becomes higher than that before the fault. This is also the same for Q factor. To verify the analysis results, a simulation is conducted using PLECS. As a result, output voltage drops after the fault because the operation characteristics change. However, by decreasing the switching frequency to match the altered resonant frequency, the output voltage is recovered to its pre-fault level.

References

[1]. F. Musavi, M. Craciun, D. S. Gautam, W. Eberle and W. G. Dunford, "An LLC Resonant DC–DC Converter for Wide Output Voltage Range Battery Charging Applications," in *IEEE Transactions on Power Electronics*, vol. 28, no. 12, pp. 5437-5445, Dec. 2013

[2]. H. Hu, X. Fang, F. Chen, Z. J. Shen and I. Batarseh, "A Modified High-Efficiency LLC Converter With Two Transformers for Wide Input-Voltage Range Applications," in *IEEE Transactions on Power Electronics*, vol. 28, no. 4, pp. 1946-1960, April 2013

[3]. X. Sun, Y. Shen, Y. Zhu and X. Guo, "Interleaved Boost-Integrated LLC Resonant Converter With Fixed-Frequency PWM Control for Renewable Energy Generation Applications," in *IEEE Transactions on Power Electronics*, vol. 30, no. 8, pp. 4312-4326, Aug. 2015

[4]. W. Martinez et al., "Three-phase LLC resonant converter with integrated magnetics," 2016 IEEE Energy Conversion Congress and Exposition (ECCE), Milwaukee, WI, USA, 2016, pp. 1-8

[5]. D. R. Linares, A. D. Expósito and M. Vasić, "High-Gain High-Frequency Three-Phase LLC Resonant Converter Design Based on the Wye–Delta Transformer for Aircraft Applications," in *IEEE Transactions on Power Electronics*, vol. 39, no. 4, pp. 4367-4383, April 2024

[6]. P. P. Nachankar, H. M. Suryawanshi, P. Chaturvedi, D. Atkar, C. L. Narayana and D. Govind, "Design of Interleaved Three-Phase DC Transformer With Ingenious Control for Modern Data Centers," in *IEEE Transactions on Industry Applications*, vol. 59, no. 6, pp. 6889-6899, Nov.-Dec. 2023

[7]. X. Guo, S. Zhang, F. Ding, J. Zhu and H. Bai, "A Novel DC–DC Converter for Electrolyzer With Low Ripple and High Step Down," in *IEEE Transactions on Industrial Electronics*, vol. 71, no. 10, pp. 12476-12486, Oct. 2024

[8]. C. Zhang, J. Wang, Y. Pan, Y. Diao and D. Li, "A DC/DC Converter for Electrolytic Hydrogen Production Based on DC Microgrid," *2022 IEEE International Power Electronics and Application Conference and Exposition (PEAC)*, Guangzhou,Guangdong, China, 2022, pp. 1348-1353

[9]. W. Zhang, D. Xu, P. N. Enjeti, H. Li, J. T. Hawke and H. S. Krishnamoorthy, "Survey on Fault-Tolerant Techniques for Power Electronic Converters," in *IEEE Transactions on Power Electronics*, vol. 29, no. 12, pp. 6319-6331, Dec. 2014

[10]. L. Ferreira Costa and M. Liserre, "Failure Analysis of the dc-dc Converter: A Comprehensive Survey of Faults and Solutions for Improving Reliability," in *IEEE Power Electronics Magazine*, vol. 5, no. 4, pp. 42-51, Dec. 2018

[11]. H. Wang, X. Pei, Y. Wu, Y. Xiang and Y. Kang, "Switch Fault Diagnosis Method for Series–Parallel Forward DC–DC Converter System," in *IEEE Transactions on Industrial Electronics*, vol. 66, no. 6, pp. 4684-4695, June 2019

[12]. B. Lu and S. K. Sharma, "A Literature Review of IGBT Fault Diagnostic and Protection Methods for Power Inverters," in *IEEE Transactions on Industry Applications*, vol. 45, no. 5, pp. 1770-1777, Sept.-oct. 2009

[13]. W. Wang, Y. Liu, P. Zhang, Y. Yuan, J. Zhao and P. C. Loh, "A Fault-Tolerant LLC Converter With High Reliability and Low Cost for Two-Stage Converters," in *IEEE Transactions on Power Electronics*, vol. 38, no. 8, pp. 9647-9659, Aug. 2023

[14]. N. Zhao, J. Liu, Y. Shi, J. Yang, J. Zhang and X. You, "Mode Analysis and Fault-Tolerant Method of Open-Circuit Fault for a Dual Active-Bridge DC–DC Converter," in *IEEE Transactions on Industrial Electronics*, vol. 67, no. 8, pp. 6916-6926, Aug. 2020

[15]. M. Berger, I. Kocar, H. Fortin-Blanchette and C. Lavertu, "Open-Phase Fault-Tolerant Operation of the Three-Phase Dual Active Bridge Converter," in *IEEE Transactions on Power Electronics*, vol. 35, no. 4, pp. 3651-3662, April 2020

[16]. W. Martinez et al., "Three-phase LLC resonant converter with integrated magnetics," 2016 IEEE Energy Conversion Congress and Exposition (ECCE), Milwaukee, WI, USA, 2016, pp. 1-8M. Noah et al., "A novel three-phase LLC resonant converter with integrated magnetics for lower turn-off losses and higher power density," 2017 IEEE Applied Power Electronics Conference and Exposition (APEC), Tampa, FL, USA, 2017, pp. 322-329

[17]. J.-Y. Lin, C.-T. Chen, K.-H. Chen, and Y.-F. Lin, "Analysis of Three-Phase Wye-Delta Connected LLC," Energies, vol. 14, no. 12, p. 3606, Jun. 2021

[18]. J. Guan *et al*., "A High Efficiency Δ-Lr-Y Type Three-Phase Interleaved LLC Converter With Less Transformer Loss," in *IEEE Transactions on*

Power Electronics, vol. 38, no. 9, pp. 11152-11168, Sept. 2023

[19]. C. Fei, R. Gadelrab, Q. Li and F. C. Lee, "High-Frequency Three-Phase Interleaved LLC Resonant Converter With GaN Devices and Integrated Planar Magnetics," in *IEEE Journal of Emerging and Selected Topics in Power Electronics*, vol. 7, no. 2, pp. 653-663, June 2019